Journal of Sound and Vibration (1999) **224**(3), 475–487
Article No. jsvi.1999.2195, available online at http://www.idealibrary.com on IDEAL®

COUPLING INTEGRAL AND GEOMETRICAL REPRESENTATIONS FOR VIBRO-ACOUSTICAL PROBLEMS

P. JEAN

Centre Scientifique et Technique du Bâtiment, 24 *rue Joseph Fourier*, 38400 *Saint Martin d'Hères*, *France*

(*Received* 20 *March* 1998, *and in final form* 14 *January* 1999)

The finite-element method is limited either to small geometries or to the low-frequency range, whereas geometrical approaches are best applied at medium and high frequencies, but do not take vibrating surfaces into account. When the vibrating boundaries of a volume are only a small part of the total boundary it is worth combining the two methods. By using geometrical methods to compute a Green function that includes all wave reflections on the surfaces of the volume, it is possible to restrict the integral representation of the pressure field to the vibrating surfaces. The surfaces to be meshed will be reduced to surfaces with known velocity fields. This approach offers a means of reducing computation times. It has been applied to large volumes corresponding to a room with a vibrating concrete wall and to a train with a vibrating window.

1. INTRODUCTION

The study of acoustical fields in closed volumes concerns not only rooms such as concert halls, but also smaller volumes in transportation vehicles such as trains, buses or cars. The first class of problem is well suited to geometrical approaches, which have proved to be convenient and precise means of predicting the solution, including binaural effects [1–3]. Fast algorithms have been developed, and the acoustical field can be computed in the medium and high-frequency ranges for volumes of arbitrary shape with locally reacting boundaries.

In the case of transportation vehicles, the acoustical field is usually coupled to vibrating surfaces which must be included in the prediction models. The finite and boundary-element techniques [4, 5] are precise ways to do this, but are limited to low frequencies. The use of an integral representation is a good means of coupling velocity and pressure fields. When the vibrating surfaces are a minor part of the total boundary, it is more computationally efficient to limit the discretized surface to the coupled boundary. Therefore, in this paper, a method consisting of an integral representation of the pressure field, combined with a geometrical approach, is proposed.

The Green functions are computed for the associated purely acoustical problem with no vibrating surfaces but with absorbent boundaries, for which

0022-460X/99/280475 + 13 $30.00/0

geometrical techniques are available. These functions must be evaluated between every nodal point on the coupled surface and the two points representing the ears of a listener. Rather than putting the source at the nodal points and the receiver at the entrances to the ears, the reverse is done, based on reciprocity. Thus, the computation is limited to two source positions. Binaural computations require the introduction of source directivities to represent the head-related transfer functions.

The proposed method [6, 7] has been validated in two cases of rectangular volumes by using the image-source method which, although time-consuming, gives results very close to the exact solution. In practice, fast computations are obtained with more sophisticated geometrical methods. The program EBINAUR [1], which combines deterministic, semi-statistical and statistical approaches, enables computation times to be significantly reduced while controlling the precision of the solution.

2. THE INTEGRAL REPRESENTATION

Figure 1 shows the geometry of the general problem P_1. The analysis is done for the harmonic time dependence $e^{-j\omega t}$. The closed volume Ω contains, on part of its boundary S, a surface S_V of known velocity V. On the remaining part of S, S_A, the boundary conditions are assumed to be locally reacting and are defined either by a mobility Y, or by an absorption coefficient α. The acoustical response in Ω is the solution of

$$(\Delta + k^2)P(M) = t(M), \tag{1}$$

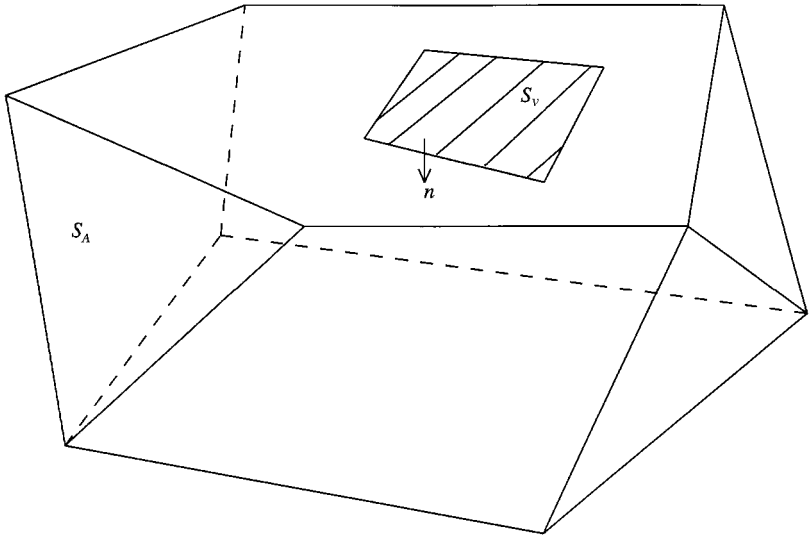

Figure 1. Geometry of the problem. n normal directed inwards volume Ω. Acoustical boundary S_A, vibrating boundary S_V.

$$\partial P(M)/\partial n = \mathrm{j}\omega\rho V(M), \quad M \in S_V, \tag{2}$$

$$V(M) = Y(M)P(M), \quad M \in S_A, \tag{3}$$

where $P(M)$ is the acoustical pressure at any point M inside Ω, k is the acoustical wavenumber, $t(M)$ is the free-field contribution at M of an acoustical source located inside the volume and n represents the normal to the boundaries directed towards the interior of Ω. V is described by an elastic linear operator which represents the behavior of S_V. If S_V is a vibrating plate, classical thin-plate theory can be used.

Using the Green integral, P can be expressed as

$$P(M) = \int_{S_V} \left[P(Q) \frac{\partial G(M,Q)}{\partial n_Q} + \mathrm{j}\omega\rho V(Q) G(M,Q) \right] \mathrm{d}S(Q)$$

$$+ \int_{S_A} \left[\frac{\partial G(M,Q)}{\partial n_Q} + \mathrm{j}\omega\rho Y(Q) G(M,Q) \right] \mathrm{d}S(Q) + t(M), \tag{4}$$

where $G(M, Q)$ is the Green solution of the problem; it gives the elementary solution at any point M for a unit point source at Q in the free field.

Now consider P_2, the problem similar to P_1, but with surface S_V assumed rigid. Let G_V be the elementary solution of this second problem: $G_V(M, Q)$ is, therefore, the pressure at any point M for a unit point source Q including all reflections on the S_A boundaries. If we introduce G_V instead of the free-field Green solution G, equation (4) reduces to

$$P(M) = \int_{S_V} \mathrm{j}\omega\rho V(Q) G_V(M,Q)\, \mathrm{d}S(Q) + t(M) \tag{5}$$

since by the definition of G_V the second integral in equation (4) is identically equal to zero on S_A and $\partial G_V/\partial n_Q$ is equal to zero on S_V.

This expression permits the introduction of a vibrating boundary into a room-acoustical problem. The use of a geometrical algorithm to compute the Green function G_V is the key idea of this approach. In general situations, geometrical methods are not valid in the low-frequency range, and this approach is, therefore, complementary to more straightforward finite-element computations [4, 5]. Furthermore, geometrical methods offer a means to reduce computation times significantly.

In equation (5) the velocity V is related to the acoustical pressure on S_V through equation (2) and the vibration of the plate is coupled to the pressure field in the volume. A simplification consists of uncoupling this problem by assuming the velocity V on S_V to be known and, therefore, not influenced by the pressure field in the volume. This assumption leads to an explicit problem instead of an implicit one. The evaluation of P with equation (5) is then straightforward.

3. NUMERICAL IMPLEMENTATION

3.1. GREEN FUNCTIONS

The evaluation of the Green function is central to this method. Several geometrical algorithms can be used. Image-source methods are easy to implement for rectangular geometries. In this particular case, and for rigid walls, it even leads to exact solutions [8], but it rapidly becomes very computationally expensive to use when the order of reflection increases. Furthermore, in practical and complex volumes with complex effects such as diffuse surface reflection, such deterministic approaches do not give the exact solution.

In the past years, dedicated techniques have been developed which permit statistical modelling which is closer to reality and results in a more accurate auralized perceived acoustics. For instance, the combination of a deterministic computation of the first reflections with a semi-statistical approach, and then a purely statistical evaluation of the reflections of higher order, is now a well-validated means of controlling both computation times and the precision of the results [1, 2]. The program EBINAUR [1], based on such a methodology, uses a variant of the cone-tracing approach for the lowest order reflections and introduces a minimum phase in the reflection coefficients. The cones do not have a finite circular cross-section, but rather an infinite Gaussian profile assuring optimized overlapping between cones. This deterministic description is used up to orders 5–10 of reflection. At higher orders, the reflections are computed in the same manner, using a statistically established set of parameters which are re-evaluated for every problem. At the highest orders of reflections, the number of contributions is high enough to be described using statistical laws. Diffuse reflection effects are included in the model. As a result of the computations, impulse responses or transfer functions are generated. The acoustical behaviour of a volume can be assessed by several criteria well known in room acoustics and it is possible to listen to the resultant auralized acoustics of any volume. The user still has the possibility to use deterministic reflections up to very high orders but, apart from a significant increase in computation times, the method will not give results closer to reality than are obtained using statistical reflections for high orders, and by modelling diffuse surface-reflection effects.

3.2. INTEGRATION

The computation of equation (5), for a known velocity field V, is done using classical discretization techniques. Surface S_V is decomposed into elements with dimensions less than or equal to one-third of the highest wavelength involved (acoustical and structural wavelengths). The velocity is known at the nodal points and linear interpolation functions are used. Each integral can be evaluated using a classical Gaussian integration technique so that, for each receiver point M, the Green functions $G_V(M, Q)$ must be computed for source points Q inside the elements. In the next examples, a simple linear integration has been used so that the G_V function are evaluated at the same nodal points as the velocity. An alternative,

based on the reciprocity principle, is to interchange the source and receiver points so that only one source at M is considered. This significantly reduces the computation times when using geometrical approaches such as EBINAUR [1]. Two source points, at the ear positions, are needed to evaluate binaural responses; head-related transfer functions are introduced as source directivities. Binaural responses must be evaluated in the time domain, either by using a Fourier transform of the pressures at the ears or by using a temporal alternative to equation (5), such as

$$p(M, t) = -\rho \int_{S_v} \gamma(Q, t)^* g_v(M, Q, t)\, \mathrm{d}S(Q) + t(M, t). \tag{6}$$

Here p, γ, t and g_v are functions of time representing the acoustical pressure, the acceleration, the source excitation and the Green function or impulse response of problem P_2.

3.3. VALIDATION PROCEDURE

The proposed method has been tested in rectangular volumes having a constant specified impedance on all parts of S_A. A known velocity is applied on S_V and the acoustical pressure is sought inside the volume. The resulting pressure on S_V is not required, since it is assumed that the velocity V is not affected by the pressure field. As a first step, the Green function has been computed using only the deterministic part of the geometrical approach: the image-sources are easy to compute in rectangular volumes and they lead to exact solutions if the walls are rigid [8]. Gensane and Santon [9] showed a very good agreement between calculations using a modal approach and a source-image calculation with plane-wave reflection coefficients, in the case of a rectangular volume with walls having real impedances. If an imaginary part was added, the agreement was not very good. Jean [10] found that, by using a spherical reflection coefficient, the correspondence between modal, finite elements and image-source calculations was very good. In the following examples, only real impedances were used and the image-source results can be considered as very precise.

In equation (5), G_V must be computed for S_V assumed rigid. At first, the computations were done omitting S_V altogether. Introduction of rigid S_V was then tested and little difference was observed. Using a spherical reflection coefficient rather than a plane-wave reflection coefficient also lead to little modifications of the results.

A modal approach [11] was used to obtain both the known velocity field on S_V and a reference solution at a chosen observation point. The modal approach can be considered as exact in the sense that it will converge towards the exact solution provided that enough modes are taken into account. In practice, this number rapidly becomes very large with increasing frequency, so that selection criteria must be used. As a result, the errors in the solution may become quite significant.

4. APPLICATION: VOLUME WITH A CONCRETE PLATE

The method is first applied to the case of a rectangular volume with dimensions $4 \times 3 \times 2{\cdot}5\,\mathrm{m}^3$. The $z = 0$ side ($4 \times 3\,\mathrm{m}^2$) is a simply supported concrete plate ($E = 28 \times 10^9\,\mathrm{N/m}^2$, $\rho = 2300\,\mathrm{kg/m}^3$, $v = 0{\cdot}15$ and thickness = 13 cm) excited by a point force of 1 N perpendicular to the surface at point $(2, 1, 0)$. The remaining walls have a specific impedance $Z = 16$ at all frequencies, corresponding to a diffuse-field absorption coefficient of 0·35 [12]. This problem is first studied using an analytical modal approach [11] in order to obtain a reference solution and the velocity field on the plate. The pressure is computed at point M $(1, 1, 1)$ by using equation (5). A 50×30 element meshing of S_V is used. This corresponds to 3·4 elements per acoustical wavelength, and 4.25 elements per flexural wavelength, of the plate at 1 kHz. An image-source method is employed to compute the Green function G_V, with plane-wave reflection coefficient and a maximum order of reflection N_r limited to 10. For a chosen value of N_r, calculations are nominally done up to N_r, but are stopped whenever the contribution of the last three orders of reflection is less than 0·2 dB. Figure 2 compares the pressure levels and phases obtained by the two methods and shows good agreement between the modal and the present integral computations.

Figure 3 represents the error in the computation of G_V as a function of N_r, at 100 and 500 Hz. In this case, the source is at receiving point M and G_V is calculated at

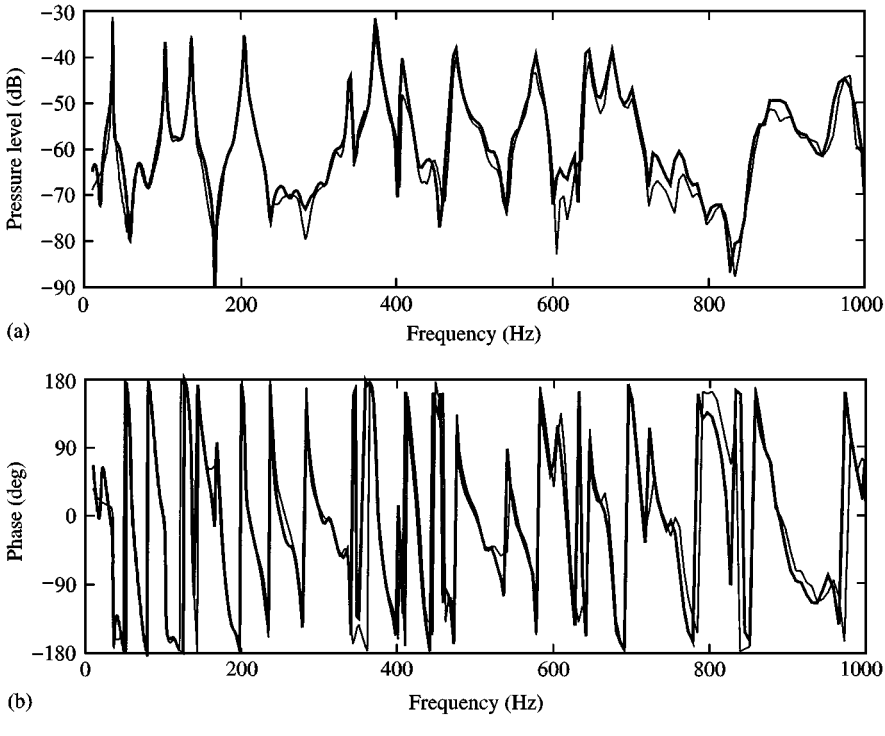

Figure 2. Sound pressure level at point $(1, 1, 1)$. (a) Level; (b) phase. —, Modal solution; ▬, integral solution $N_r = 10$.

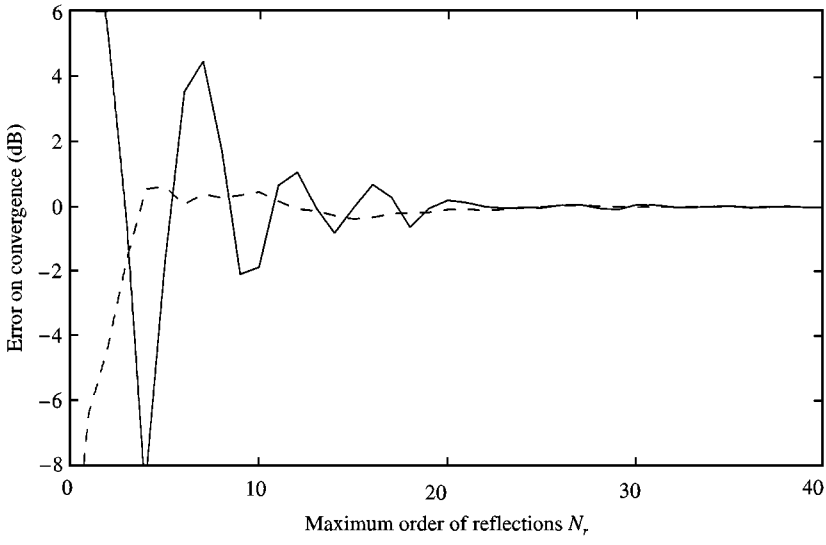

Figure 3. Convergence of G_V. Unit monopole at (1, 1, 1) and receptor at the centre of the plate (2, 1·5, 0). —, 100 Hz; - - -, 500 Hz.

the centre of the concrete plate. The computational error was obtained by referring the calculations to results obtained with $N_r = 200$. Although full convergence is not achieved with $N_r = 10$, the final results of Figure 1 compare well with the reference solution, even at low frequencies. The parallelepiped is a particular case for which geometrical methods converge even at low frequencies, provided that sufficient reflections are considered.

5. APPLICATION: CASE OF AN ELONGATED VOLUME WITH A WINDOW

The second application concerns a volume with dimensions close to those of a train coach. Figure 4 shows the geometry of the problem. The coach has dimensions of $10 \times 2{\cdot}2 \times 2$ m^3 and one side has a glass window simply supported on all sides. This window is 5 mm thick and has dimensions $1{\cdot}2 \times 0{\cdot}8$ m^2 with $E = 64 \times 3\ 10^9$ N/m^2, $\rho = 2500$ kg/m^3 and $\nu = 0{\cdot}15$. It is positioned 0·7 m above the ground, 1·9 m away from the end of the car and is excited at point P (5·88, 0·7,0) by a force of 1 N perpendicular to the surface. A receiver point M at (6·4, 0·9, 1·15) is considered. A 30×20 element meshing of S_V is used, corresponding to 4·25 elements per acoustical wavelengths, and 3·81 elements per flexural wavelength of the plate, at 2000 Hz.

5.1. ABSORBENT CONDITIONS

As a first step, all parts of S_A have a specific impedance of $Z = 16$ as in the previous example and the rate of convergence of G_V is similar to that obtained in

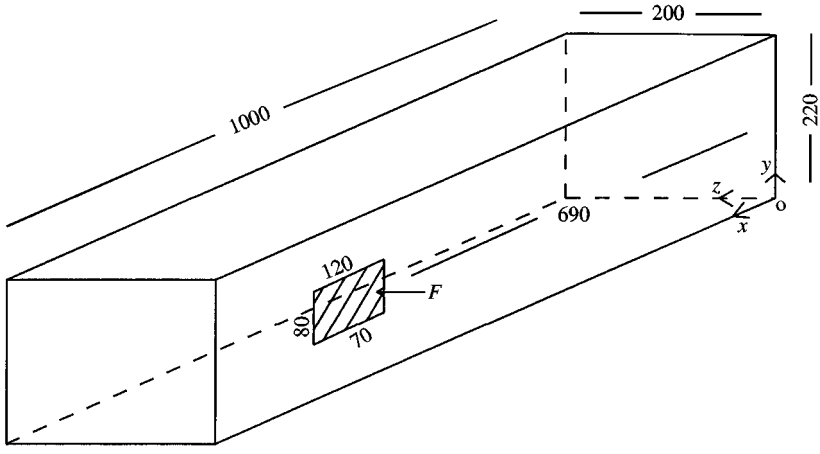

Figure 4. Geometry of the train with a window Distances in cm. Unit force F at (7·08, 1·04, 0). Observation point at (6·4, 0·9, 1·15).

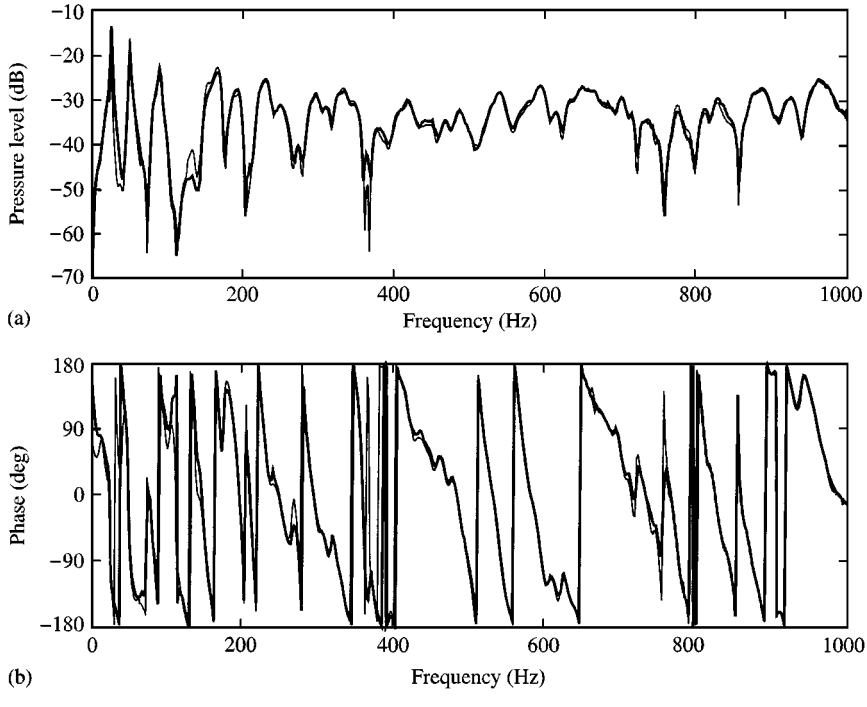

Figure 5. Sound pressure level at point (6·4. 0·9, 1·15). Absorbent conditions, 0–1000 Hz. (a) Level; (b) phase. —, Modal solution; ▬, integral solution $N_r = 10$.

Figure 3. In Figures 5 and 6, the modal and present solutions are compared, first below 1000 Hz and then between 1000 and 2000 Hz. The computations of G_V was done up to $N_r = 10$; a very good agreement is then obtained. Above 1000 Hz, the agreement is slightly degraded. It has been established that convergence of the

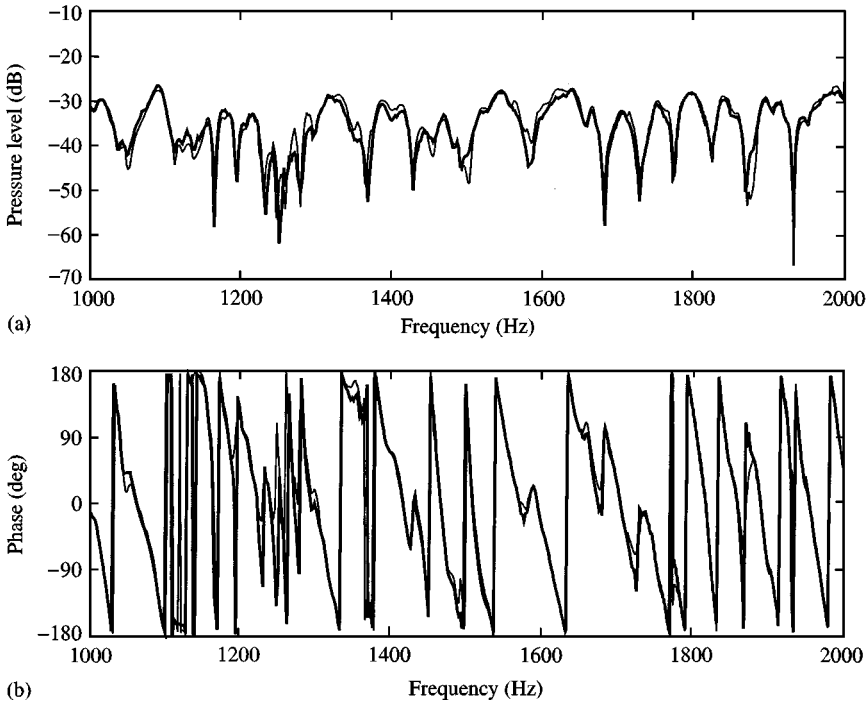

Figure 6. Sound pressure level at point (6·4, 0·9, 1·15). Absorbent conditions, 1000–2000 Hz. (a) Level; (b) phase. —, Modal solution; ▬, integral solution $N_r = 10$.

modal solution was not yet achieved in this frequency range; this could not be further improved, due to a limit in the memory capacity of the computer that was used. Conversely, the image-source solution has reached convergence with $N_r = 10$ and calculations with $N_r = 20$ did not show any significant difference. The meshing also seems sufficient since, even at 2000 Hz, a good comparison is obtained.

5.2. 'REVERBERANT' CONDITIONS

All the surfaces in the volume have now diffuse-field absorption coefficients of 0·065, 0·073, 0·09, 0·107 and 0·115 in the octave bands 125, 250, 500, 1000 and 2000 Hz respectively. The convergence of G_V, at the centre of the window, with the maximum order of reflections N_r is plotted in Figure 7. Due to a lower absorption than in the previous case, the solution converges for higher values of N_r—typically above $N_r = 40$.

Figures 8 and 9 compare, for two selected frequency ranges, the pressure field at M computed by the two methods with the maximum order of reflection limited to $N_r = 40$. Again, good agreement is obtained with $N_r = 40$, especially for the phase. Zoomed frequency ranges have been presented for the sake of clarity, but results at other frequencies are equally good.

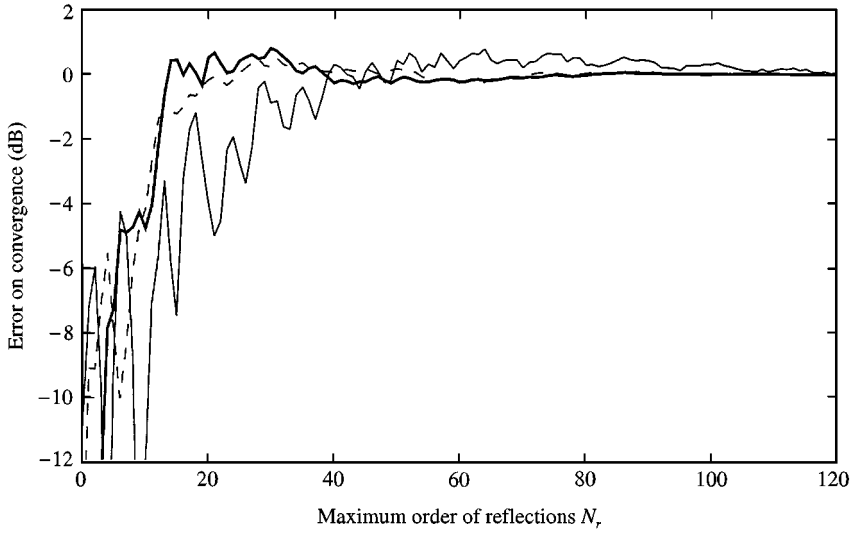

Figure 7. Convergence of G_V. Unit monopole at (6·4, 0·90, 1·15) and receptor at the centre of the window. —, 100 Hz; - - -, 500 Hz; ▬, 2000 Hz.

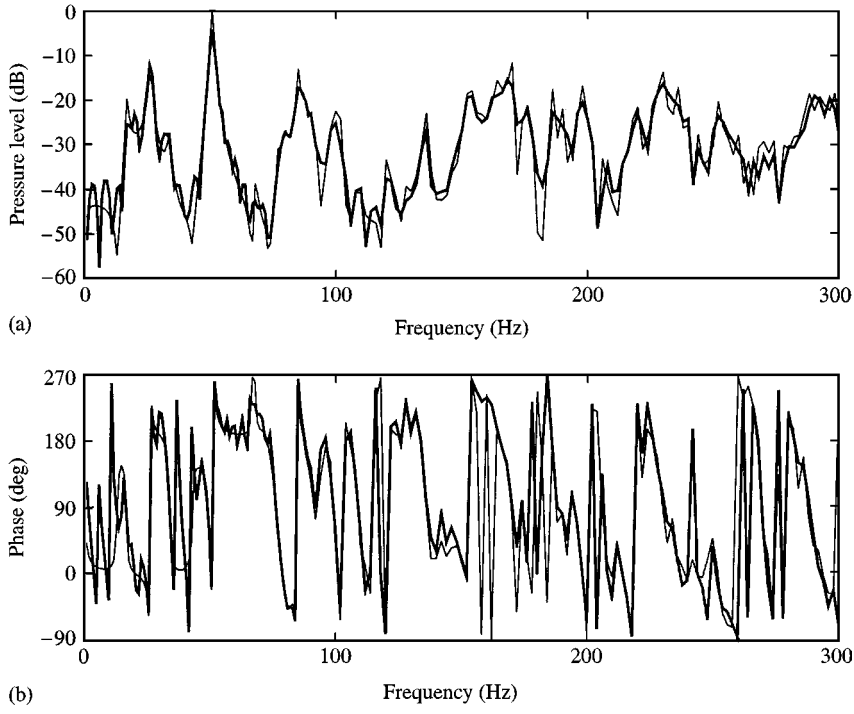

Figure 8. Sound pressure level at point (6·4, 0·9,, 1·15). Reverberant conditions, 0–300 Hz. (a) Level; (b) phase. —, Modal solution; ▬, integral solution $N_r = 40$.

Finally, Figure 10 compares the modal and integral solutions ($N_r = 10$ and 40) in third-octave bands, showing the improvement when N_r is increased. The differences remaining between the modal and the integral approaches can be partly attributed

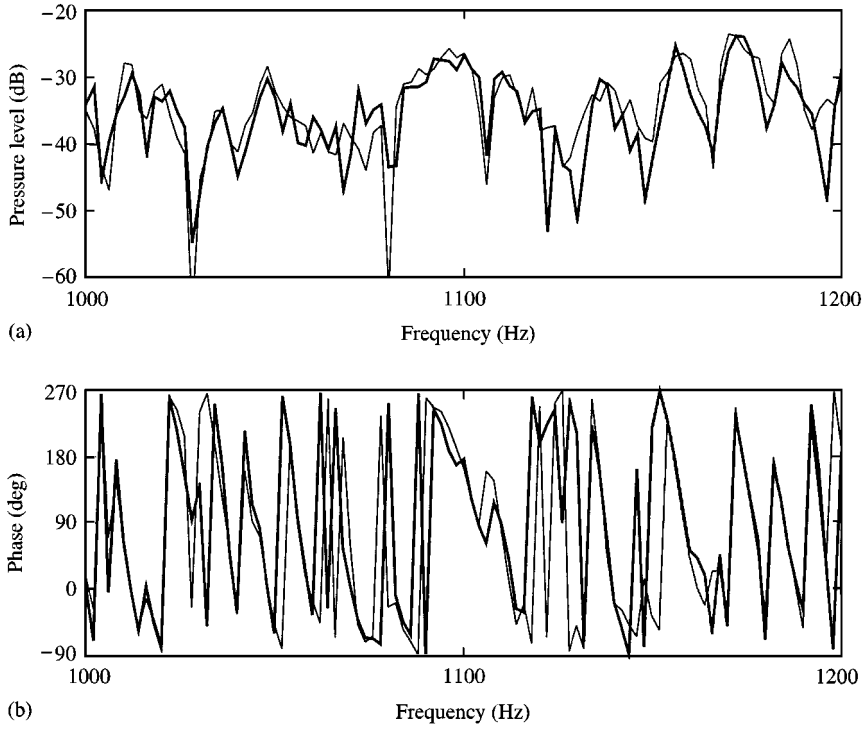

Figure 9. Sound pressure level at point (6·4, 0·9, 1·15). Reverberant conditions 1000–1200 Hz. (a) Level; (b) phase. —, Modal solution; ▬, integral solution $N_r = 40$.

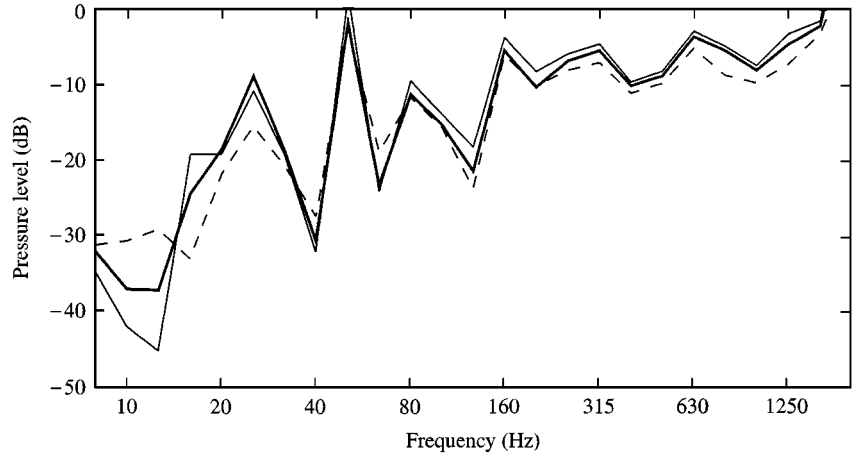

Figure 10. Sound pressure level at point (6·4, 0·9, 1·15). Third-octave bands. —, modal solution; - - -, integral solution $N_r = 10$; ▬, integral solution $N_r = 40$.

to an insufficient value of N_r. In the light of the results obtained for a more absorbent volume—and since the image-source method is, in theory, more precise for reverberant media—it can be inferred that the modal calculations are also

somewhat approximate, since only a selection of the modes is retained in the computation. At higher frequencies (Figure 9 compared to Figure 8) the agreement between the modal and the integral results is not as good as for lower frequencies. Again, an insufficient number of modes might explain this difference.

6. CONCLUSION

An integral representation has been used to compute pressures in volumes with a vibrating boundary of known velocity. The integral is evaluated only on the vibrating surface, and the acoustical volume effect is included in the Green function. With this approach it is possible to solve problems in the medium- and high-frequency ranges, since the Green function can be evaluated with efficient geometrical approaches. It is clear that this technique is mainly of interest in cases when the vibrating boundary is a limited portion of the total surface of the volume. The fact that prerequisite knowledge of the velocity field is required assumes that the pressure field does not significantly influence the behaviour of the vibrating surfaces. This approach could be used, for instance, in the case of a train or an aircraft, in which one or several windows contain a velocity field due to exterior air flow, and when another model can be used to estimate this input velocity field. Machines or engines radiating noise in enclosures could be first studied using a finite-element technique, deducing velocity fields thereafter used as input to the proposed method. The reciprocity principle enables the receiver and source positions to be interchanged so that only one source position need be considered at each receiver point. The method has been validated in the case of a building problem, and for a train-coach configuration with a vibrating window. The objective of the computations presented here was to verify the convergence of the method; an image-source method has been used to calculate the necessary Green functions. It is a computationally expensive way of evaluating the Green functions, since all reflections up to a given order are taken into account in a deterministic way. Computations using the optimised algorithms of the EBINAUR program permit deterministic, semi-statistical and statistical approaches to be combined. Calculations have shown that similar results are obtained with this program. Complex shapes with diffusely reflecting surfaces can be studied, and the introduction of ear transfer functions enables the computation of binaural effects necessary to accurately evaluate the perceived acoustical quality of volumes such as cars, aeroplanes or trains.

ACKNOWLEDGMENT

The author expresses his gratitude to the Région Rhône-Alpes [6] which funded the preliminary development of this work. L. Gagliardini, as well as the acoustical team of the CSTB, should also be thanked for fruitful discussions which originated this work.

REFERENCES

1. J. Martin, D. Van Maercke and J. P. Vian 1993 *Journal of the Acoustical Society of America* **94**, 3255–3264. Binaural simulation of concert halls: a new approach for the binaural reverberation process.
2. J. P. Vian and J. Martin 1992 *Applied Acoustics* **36**, 293–305. Binaural room acoustics simulation: practical uses and applications.
3. M. Emerit, E. Dudouet and J. Martin 1995 *15th ICA Trondheim* **2**, 437–440. Head related transfer function and high order statistics.
4. P. Jean 1985 *Thèse de doctorat*, *Universitè de Technologie de Compiègne*. Une méthode variationnelle par équations intégrales pour la résolution de problèmes intérieurs et extérieurs de couplage élasto-acoustique. (english version available upon request).
5. P. Jean and M. A. Hamdi 1985 *Colloque tendances actuelles en calcul des structures*, *Bastia*, *6–8 Novembre*. Résolution numérique des problèmes couplés par une méthode d'éléments finis de frontière.
6. P. Bruder, L. Gagliardini, P. Jean and J. P. Vian 1997 *Convention Actra No.* 125740000. Confort acoustique dans les moyens de transport.
7. P. Jean, J. Martin and J. P. Vian 1998. *Séminaire Confort acoustique et vibratoire automobile et ferroviaire*, *Courbevoie 3 et 4 Decembre*. Couplage vibro-acoustique à l'aide d'une approche d'acoustique géométrique.
8. J. B. Allen and D. A. Berkeley 1979 *Journal of the American Society of Acoustics* **65**, 943–950. Image method for efficiently simulating small-room acoustics.
9. M. Gensane and F. Santon 1979 *Journal of Sound and Vibration* **63**, 97–108. Prediction of sound fields in rooms of arbitrary shape: validity of the image sources method.
10. P. Jean 1990 Internal Report, *Centre Scientifique et Technique du Bâtiment*. Comparaison de trois méthodes pour l'étude du comportement d'un volume avec conditions d'impédances.
11. L. Gagliardini, J. Roland and J. L. Guyader 1991 *Journal of Sound and Vibration* **145,** 457–478. The use of a functional basis to calculate acoustic transmission between rooms.
12. P. M. Morse and K. U. Ingard 1986 *Theoretical Acoustics*, p. 580. *Princeton*, *NJ*: *Princeton University Press.*